Absence of Germanate Anomaly in Ternary Lithium Germanophosphate Glasses: Modification Behavior of Mixed Glass System of Strong and Fragile Formers

Sundeep Kumar, S. Murugavel, and K. J. Rao*

Solid State and Structural Chemistry Unit, Indian Institute of Science, Bangalore 560 012, India

Received: October 10, 2000; In Final Form: April 9, 2001

Ternary lithium germanophosphate glasses have been synthesized over a wide range of compositions. Thermal and spectroscopic techniques (IR, Raman, and ^{31}P MAS NMR) have been used to investigate their properties and structures. It is found that modification occurs almost exclusively on the P_2O_5 part of the structure and the GeO_2 network appears unaffected. $GeO_{6/2}$ octahedra are not formed in the glasses, except in one GeO_2-rich and Li_2O-poor composition. Thermodynamic arguments are given to rationalize this behavior. The unique behavior of the T_g values and molar volumes have been discussed in terms of a model, which considers modification occurring only on the P_2O_5 part of the glass structure. $F_{1/2}$ fragilities of these glasses have been evaluated from ΔT_g and T_g values, and a relation between $F_{1/2}$ and the physical dimensionality has been proposed.

1. Introduction

Germanate glasses have potential industrial applications and therefore have been investigated fairly extensively.[1−7] The so-called germanate anomaly, exhibited by binary germanate glasses, is also a fascinating phenomenon, which occurs in binary alkali germanate glasses. It originates from the tendency of germanium to form octahedral coordination to oxygen in a limited range of compositions in addition to its normal tetrahedral coordination. This composition-dependent change in coordination of germanium leads to the incidence of extrema in several physical properties such as density, molar volume, and refractive index. Murthy and Kirby[1] were among the first to observe the manifestation of this anomaly in the IR spectra of alkali germanate glasses, where the 880 cm^{-1} absorption due to Ge−O−Ge was found to red shift as a function of alkali oxide concentration and exhibit a maximum shift of ∼100 cm^{-1} around 30 mol % alkali. The red shift was attributed to the reduction of the relevant force constant due to the formation of $GeO_{6/2}$ units in the glass. Sakka and Kamiya[2] confirmed this observation in the EXAFS and XRD studies, while noting that the maximum shift in the Ge−O−Ge absorption peak and the change in Ge−O distances occur around 20 mol % alkali. The occurrence of minima in the properties of binary alkali germanate glasses has been reported in several studies,[1−7] although the composition corresponding to the minimum depends on the alkali. The presence of six-coordinated Ge has also been reported to influence Na^+ ion transport in aluminogermanate glasses.[3]

The origin of the germanate anomaly has, however, also been attributed by Henderson and Fleet[8] to the formation of small three-membered rings of $GeO_{4/2}$ tetrahedra. These authors have argued that the absence of the 700 cm^{-1} peak, typical of six-coordinated Ge, observed in the spectra of GeO_2 of rutile structure and the increase in the intensity of 515 cm^{-1} vibrational band in the Raman spectra indicate that the presence of rings is responsible for the observed phenomenon. Nevertheless, Jain and co-workers[9−11] have shown through combined EXAFS and XPS studies that both octahedrally coordinated Ge and non-bridging oxygens (NBOs) are present in the region of the germanate anomaly. The concentrations of both $GeO_{6/2}$ and NBOs increase up to 20 mol % modifier. NBOs continue to increase at the expense of $GeO_{6/2}$ above this concentration. Jain et al.[9] attribute the germanate anomaly to the variations in the "unoccupied volume" of the glass structure. Further EXAFS studies of Osaka et al.[12] revealed the formation $GeO_{6/2}$ octahedra in the GeO_2−TeO_2 system, where both GeO_2 and TeO_2 are known to be glass formers. They suggested that the germanate anomaly in these glasses is due to the formation of $GeO_{6/2}$ octahedra rather than small rings of the type of Ge_3O_9 described by Henderson and Fleet.

Extensive Raman and IR studies have been reported by Kamitsos et al.[13,14] on rubidium germanate glasses. These authors have concluded that the spectra are consistent with the formation of $GeO_{6/2}$ octahedra which above 15 mol % Rb_2O reverts to the conventional modification and formation of NBOs. Raman spectra of GeO_2 glass at high pressures have been studied,[15] and the presence of units such as Ge_4O_{16} and of interconnected $GeO_{4/2}$ and octahedral $GeO_{6/2}$ have been noted. The formation of $GeO_{6/2}$ octahedra up to 20 mol % alkali is also supported by neutron scattering studies of Price et al.,[16] who also find a continuous increase in NBOs in the same compositions. In the well-focused investigation of the problem of six-coordinated Ge by Hussin et al.[17] it was found that the formation of NBOs is rather negligible below 10 mol % Na_2O, and the dominant effect is only the formation of octahedrally coordinated germanium.

The requirement for the formation of $GeO_{6/2}$ is the availability of oxygen for increased bonded coordination, which is provided by the modifier oxides. The eventual breakdown of these additional Ge−O bonds and formation of NBOs above a certain concentration of the modifier oxide suggest that octahedra become unstable and revert to tetrahedra above a critical concentration of the $GeO_{6/2}$ in the structure. It would therefore be interesting to examine the physicochemical factors behind this instability. The problem does not appear to have been

* Corresponding author. Phone: +91-80-309 3583. Fax: +91−80−360 1310; +91−80−360 0683.

10.1021/jp0036386 CCC: $20.00
Published on Web 06/01/2001

TABLE 1: Compositions, Codes, Densities, and Molar Volumes of $Li_2O-GeO_2-P_2O_5$ Glasses

	composition				
sample	Li_2O (x)	GeO_2 (y)	P_2O_5 (z)	density (g/cm^3)	V_M (cc)
CPL1	0.10	0.50	0.40	3.28	34.16
CPL2	0.20	0.40	0.40	3.07	34.07
CPL3	0.30	0.30	0.40	2.99	32.48
CPL4	0.40	0.20	0.40	2.84	31.57
CPL5	0.50	0.10	0.40	2.60	31.61
CLG0	0.50	00	0.50	2.35	36.56
CLG1	0.50	0.05	0.45	2.45	34.30
CLG2	0.50	0.10	0.40	2.60	31.61
CLG3	0.50	0.15	0.35	2.65	30.30
CLG4	0.50	0.20	0.30	2.73	28.73
CGP1	0.50	0.20	0.30	2.73	28.73
CGP2	0.40	0.20	0.40	2.84	31.57
CGP3	0.30	0.20	0.50	2.76	36.54

examined using ternary glasses containing GeO_2. The oxygen provided by the modifier oxide could be preferentially taken away by another competing network former in a suitably formulated ternary glass, in which case germania should be expected to remain simply tetrahedral unless there is a more dominant structural reason for the formation of octahedra. In the binary GeO_2-TeO_2 glasses, however, the formation of GeO_6 octahedra noted by Osaka et al.[12] suggests that there is a pronounced tendency toward the formation of $[GeO_{6/2}]^{2-}$ units in any glass containing GeO_2.

To investigate this problem, germanophosphates would provide such a glass system from the known chemical trends in silicophosphate glasses.[18] We expect P_2O_5 to compete with GeO_2 for the O^{2-} ion from the modifier oxide. This could leave the tetrahedral structure GeO_2 in the glass unaffected. With this expectation, we have examined the thermal properties and vibrational and MAS NMR spectra of lithia-modified germanophosphate glasses over a fairly wide range of compositions. We observe that in germanophosphate glasses the tendency to form $GeO_{6/2}$ octrahedra is greatly suppressed due to the higher acidity of P_2O_5, which takes up all the O^{2-} ions of the modifier oxide.

The glasses also provide a new perspective since they can be viewed as a pseudo binary glass consisting of a rather "strong" GeO_2 and a rather "fragile" lithium phosphate. We have examined the glasses from this viewpoint also. On the basis of a plausible new relation between the kinetic $F_{1/2}$ fragilities[19] of these glasses and their spatial dimensionalities, we find further indication that GeO_2 in the glass structure remains unmodified.

2. Experimental Section

Glasses were prepared by the conventional melt quenching method using analytical reagent (AR) grade GeO_2 (Aldrich), Li_2CO_3 (Qualigens), and $(NH_4)_2HPO_4$ (BDH laboratory reagent) as starting materials. Calculated quantities of starting materials were mixed well by grinding them together to a fine powder. The powders were heated in platinum crucibles at 573 K for about 5 h in a muffle furnace to decompose $(NH_4)_2HPO_4$ to P_2O_5. The temperature was raised to 1000 K when Li_2CO_3 also decomposes to Li_2O. The batches were then melted at 1623 K for about 10 min in a Thermolyne furnace, stirred to ensure homogeneity, and quenched between stainless steel plates kept at room temperature. The nominal compositions of all the glasses prepared in this manner and their designations are listed in Table 1. The glasses have been grouped in three categories based on the constancy of the mole fraction of one of the components. Some of the compositions find duplicate entries in different categories as they belong to both groups. The glasses were all transparent and colorless.

The amorphous nature of the samples was confirmed using X-ray diffraction (JEOL JOX-8P X-ray diffractometer). The glassy nature was ascertained and the glass transition temperatures (T_g) of the samples were determined using a differential scanning calorimeter (Perkin-Elmer DSC-2). Dry nitrogen was used as purge gas in the DSC measurements. The glasses were annealed at (T_g − 20) K for about 3 h in each case. The heat capacities of the annealed glasses were determined from room temperature to temperatures well above T_g (limited only by the incidence of crystallization) using single-crystal sapphire (Al_2O_3) as a heat capacity standard. The heating rate used was 10 degree/minute. The densities were determined using glass pieces free of air bubbles and cracks (visual examination) through apparent weight loss method. Xylene was used as the immersion fluid. The molar volumes, $V_m = W_m$/density, were calculated from density data, where W_m is the formula weight.

The FTIR spectra of the glasses were recorded between 4000 and 400 cm^{-1} on a Perkin-Elmer Spectrum 1000 FTIR spectrometer. KBr pellets containing glasses were prepared by standard processes described elsewhere.[20] Raman spectra were recorded on a Spex 1403 Raman spectrometer using 514.5 nm radiation from an argon ion laser (Spectra-Physics Series 2000). All of the spectra were recorded at room temperature (293 K) on large glass bits. The laser power used was 0.40 W. The increment was 1 cm^{-1} and integration time was 0.5 s. The data were collected at 90° − reflection mode using a water-cooled photomultiplier tube (PMT). ^{31}P MAS NMR spectra were recorded on a Bruker MSL-300 solid-state high-resolution spectrometer operating at 90.4 MHz (magnetic field 7.05 T). 90° pulses of 5 μs were employed with a delay time of 10 s between pulses in all of the experiments. A spinning speed of 3−7 kHz was employed. All of the spectra were recorded at room temperature using freshly powdered samples.

3. Results and Discussion

We first propose a heuristic model for the modification of germanophosphate glasses by Li_2O, assuming that GeO_2 and P_2O_5 form a random network. The electronegativities of the glass-forming oxides are used as guides to determine the course of modification. The compositional boundaries for the formation of various structural species is thus established. We then discuss the observed properties of the glasses in the present system in the light of the model.

3.1. Structural Model. The random network of $GeO_2-P_2O_5$ glass can be considered as built from primary structural units, $[GeO_{4/2}]^0$ and $[PO_{3/2}]^0$. GeO_2 and P_2O_5 provide these structural units, $GeO_2 \equiv [GeO_{4/2}]^0$ (represented as G_4) and $P_2O_5 \equiv 2[PO_{3/2}]^0$ (represented as $2P_3$), respectively. When these units are randomly connected in the glass, P−O−Ge, P−O−P, and Ge−O−Ge bond segments are formed at random. Because of the differences in electronegativities, χ, of the structural units $[GeO_{4/2}]^0$ and $[PO_{3/2}]^0$ ($\chi_{G4} = 2.875$, $\chi_{P3} = 3.023$), heterogroup connectivities (G_4 being connected preferentially to P_3 and vice versa) may be assumed to dominate. The result is that P−O−Ge bridges are formed in preference to P−O−P or Ge−O−Ge bridges. When present in stoichiometric proportion, GeO_2:P_2O_5 :: 3:2, only P−O−Ge bonds are expected to be present. When P_2O_5 is in excess of this proportion, there will be P−O−P bonds in addition to P−O−Ge bonds. It may be noted from Table 1 that GeO_2 and P_2O_5 concentrations are such that we expect only P−O−Ge and P−O−P bonds to be present in the glasses investigated here. When Li_2O is added in order to modify the structure, it implies that O^{2-} ions react with bridging oxygens. Between the P−O−P or P−O−Ge bridges, the O^{2-} ion is

directed toward that bridge, which offers lower net barrier for approach. P−O−Ge offers a lower barrier compared to P−O−P, because the partial charges on the atoms in P−O−Ge and P−O−P are as shown below.

bond	connectivity of bonds	partial charges on atoms in the links			electronegativity of the units
		P	O	Ge	
P−O−P	P_3P_3	0.361	−0.144	−	3.023
P−O−Ge	P_3G_4	0.331	−0.168	0.427	2.953

O^{2-} ion experiences lower barrier while approaching a P−O−Ge (repulsion plus attraction) than while approaching a P−O−P segment. The result of modification is the formation of $[POO_{2/2}O]^{-1} \equiv P_2$ and $[GeO_{3/2}O]^{-1} \equiv G_3$.

$$[POO_{3/2}]^0 + [GeO_{4/2}]^0 + O^{2-} \rightarrow [POO_{2/2}O]^{1-} + [GeO_{3/2}O]^{1-}$$

$$P_3 + G_4 + O^{2-} \rightarrow P_2 + G_3 \quad (1)$$

Indeed use of bond energy hierarchies as basis for modification (weaker bond being modified in preference) leads to identical results as shown by us elsewhere.[21] In the above representation it is assumed that the reacting units are connected by P−O−Ge bonds which are modified to $P-O^-$ and $Ge-O^-$. If the resulting G_3 is connected to another P_3, which is very likely in the present system of phosphate rich glasses, a second reaction occurs readily. This is a bond switching reaction of the type

$$P_3 + G_3 \rightarrow G_4 + P_2 \quad (2)$$

This reaction is driven by the difference in the electronegativities of G_3 and P_3, which is the equivalent to a local free energy difference. The electronegativities of the four species P_2, P_3, G_3, G_4 are respectively 2.391, 3.023, 2.189, 2.875. The above bond-switching reaction results in a reduction of the difference in electronegativities of neighboring groups, which is the chemical driving force for the reaction. We further note that these electronegativities and partial charges have all been calculated using Sanderson's procedure,[18,21−24] which is based on the application of the electronegativity equalization procedure. The net reaction, which is a sum of reactions 1 and 2, suggests that modification results in the formation of only metaphosphate units and $[GeO_{4/2}]^0$ is left unaffected. Since the P_2O_5/GeO_2 ratio is greater than 2/3 in all the glasses studied here the, availability of P_3 units in the immediate neighborhood of G_3 can be safely assumed. As the Li_2O content is increased to a level where the Li_2O/P_2O_5 ratio is greater than 1, G_3 will not be able to find a P_3 to enable reaction 2 to occur, and this should result in the retention of G_3 in the structure. Subsequent reaction can be only of the type

$$[POO_{2/2}O]^{1-} + [GeO_{4/2}]^0 + O^{2-} \rightarrow [POO_{1/2}O_2]^{2-} + [GeO_{3/2}O]^{1-}$$

$$G_4 + P_2 + O^{2-} \rightarrow G_3 + P_1 \quad (3)$$

Because the earlier stages of modification would have already established many P_2-P_2 (P−O−P bridges) connectivities at the expense of P_3-G_4 (P−O−Ge bridges) connections, we expect

$$2P_2 + O^{2-} \rightarrow 2P_1 \quad (4)$$

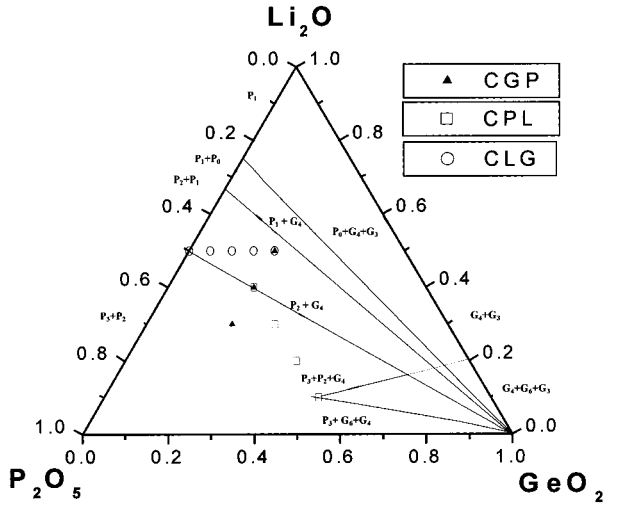

Figure 1. The ternary phase diagram for $Li_2O-GeO_2-P_2O_5$ system. Compositions investigated are indicated by symbols. The lines delineate the nature of structural species in the glass. The dotted line intersecting the P_2, P_1, and P_0 lines is only to suggest that the terminus of this line is at 20% GeO_2. No literature data is available in this range to fill the structural phase diagram.

type of reactions. Reactions of the type

$$2G_4 + O^{2-} \rightarrow 2G_3 \quad (5)$$

may not occur because the added Li_2O is likely to be driven more into the modified, more acidic, and more ionic phosphate sites than to GeO_2 (dominated) sites in the structure. Reaction 4 dominates at this stage of modification. The nature of modification in germanophosphate glasses is, therefore, expected to be very similar to those that occur in silicophosphate glasses,[18] except for the complications that arise if $[GeO_{6/2}]^{2-}$ units are formed in the glasses. The model results are presented as a structural phase diagram[25] in Figure 1, where regions are bounded by the nature of the structural species. The actual composition of glasses studied in this paper are also indicated. To our knowledge the glass formation region in this system has not been reported.

3.2. Formation and Stability Regime of $[GeO_{6/2}]^{2-}$. Formation of $[GeO_{6/2}]^{2-}$ units cannot be ruled out in the initial stages of modification in view of the literature reports cited in the Introduction. We propose that formation of $[GeO_{6/2}]^{2-}$ is facile only when (i) two Ge atoms are structurally close to each other and (ii) there is a thermodynamic advantage in converting modifier O^{2-} ion into a bridging oxygen as in $[GeO_{6/2}]^{2-}$ units, rather than to the NBOs. The first requirement is met only in GeO_2-rich glasses. The entropic advantage in the formation of two NBOs per O^{2-} ions is obvious, as these are P_2O_5-rich glasses and there are more sites for modification. But then the formation of two Ge−O bonds may be energetically more advantageous because two P−O bonds in P−O−P are expected to be stronger than two $P-O^-$ bonds. This is so because of the correlation term arising from an additional electron in the resulting lone pairs in a $P-O^-$ bond.

To examine this suggestion semi qualitatively, we consider the following two competitive reactions:

$$[GeO_{4/2}]^0 + Li_2O \rightarrow [GeO_{6/2}]^{2-} + 2Li^+ \quad (I)$$

$$2[POO_{3/2}]^0 + Li_2O \rightarrow 2[POO_{2/2}O]^{1-} + 2Li^+ \quad (II)$$

The respective free energy changes, ΔG_1 and ΔG_{II}, can be

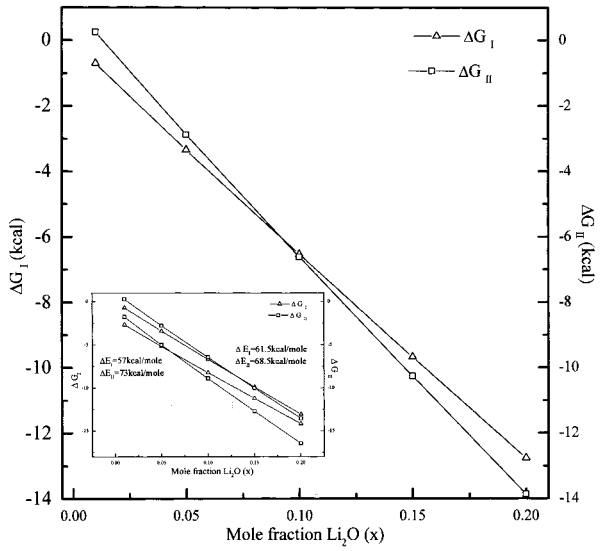

Figure 2. Variation of free energies (ΔG) calculated for reactions I and II as a function of mole fraction of Li_2O for the cases where Ge is present in octahedral and tetrahedral coordinations. The inset shows the error limits to this evaluation. In the inset, ΔG is calculated with ΔE values of 57 and 73 kcal/mol and are shifted by −2 kcal for clarity.

written as

$$\Delta G_{\mathrm{I}} = \Delta H_{\mathrm{I}} - T\Delta S_{\mathrm{I}}^{\mathrm{C}} \approx \Delta E_{\mathrm{I}} - T\Delta S_{\mathrm{I}}^{\mathrm{C}}$$

$$\Delta G_{\mathrm{II}} = \Delta H_{\mathrm{II}} - T\Delta S_{\mathrm{II}}^{\mathrm{C}} \approx \Delta E_{\mathrm{II}} - T\Delta S_{\mathrm{II}}^{\mathrm{C}}$$

where $S_{\mathrm{I}}^{\mathrm{C}}$ and $S_{\mathrm{II}}^{\mathrm{C}}$ are the configurational entropies. We have deliberately ignored both $P\Delta V$ and vibrational entropy terms, as they are generally of much lower in magnitude[26] and are present in roughly equal measure in both the reactants and products in the two reactions. The configurational entropy terms $S_{\mathrm{I}}^{\mathrm{C}}$ and $S_{\mathrm{II}}^{\mathrm{C}}$ are given by

$$S_{\mathrm{I}}^{\mathrm{C}} = -m_1 R[x_1 \ln x_1 + (1-x_1)\ln(1-x_1)]$$

$$S_{\mathrm{II}}^{\mathrm{C}} = -m_2 R[2x_2 \ln x_2 + 2(1-x_2)\ln(1-x_2) + 2\ln 2]$$

where x_1 and x_2 are the mole fractions of Li_2O in the pseudo binaries, $xLi_2O-yGeO_2$ and $xLi_2O-zP_2O_5$ identifiable in the ternary glasses $xLi_2O-yGeO_2-zP_2O_5$. The quantities x_1 and x_2 are given by the expressions $x_1 = x/(x+y)$ and $x_2 = x/(x+z)$ because

$$xLi_2O-yGeO_2 = (x+y)\,[\,x/(x+y)\,Li_2O - y/(x+y)\,GeO_2\,] \equiv m_1\,[x_1\,Li_2O - (1-x_1)\,GeO_2\,]$$

where $m_1 = (x+y)$ and $x_1 = x/(x+y)$.

Similarly, $xLi_2O-zP_2O_5 \equiv m_2[x_2Li_2O - (1-x_2)P_2O_5]$, where $m_2 = (x+z)$ and $x_2 = x/(x+z)$. ΔE_{I} and ΔE_{II} are unfortunately not available for the various compositions. Therefore, we make an approximate estimate of the energy values using the expression $\Delta E = -30|\Delta\chi|^2$, where $\Delta\chi$ is equal to the difference in the electronegativities of the reactants, in the spirit of Pauling's thermochemical definition of electronegativities.[27] χ is treated as group electronegativity and taken as a geometric mean of the electronegativities of the constituent atoms. For example, $\chi_{GeO4/2} = [\chi_{Ge}.(\chi_O)^2]^{1/3}$. Using group electronegativities ($\chi_{G4} = 2.875$, $\chi_{Li2O} = 1.497$, $\chi_{P3} = 3.023$.), the molar energies of the reactions I and II are approximately 60 and 70 kcal per mole, respectively. ΔG has been calculated from above expression, and, in Figure 2, we show the behavior of ΔG_{I} and ΔG_{II} as a function of Li_2O concentration. It shows that below ~8% Li_2O, lower free energy indicates stability of $[GeO_{6/2}]^{2-}$ units. In Figure 1, the region of $[GeO_{6/2}]^{2-}$ formation is indicated by a line open at one end. It must be noted that the energies used are approximate and the intersection of the two free energy lines occurs at 6%, when the ΔE_{I} and ΔE_{II} used are 57 and 73 kcal/mol, respectively, whereas it is 12.5% if ΔE_{I} and ΔE_{II} used are 61.5 and 68.5 kcal/mol, respectively (see inset to Figure 2). This represents approximately the error limits to this evaluation.

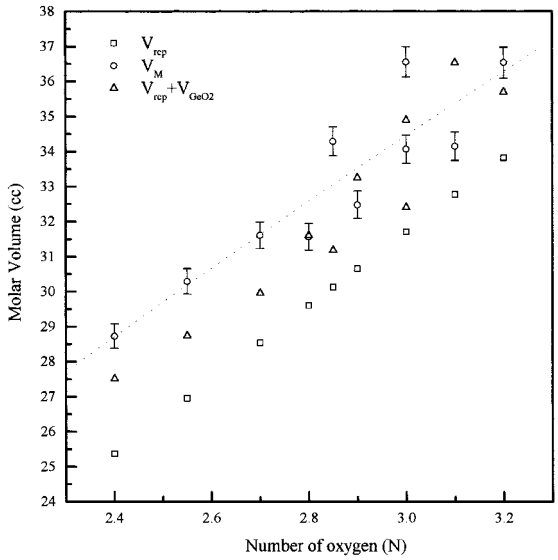

Figure 3. Variation of molar volume as a function of number of oxygens in the glass compositions.

We now discuss various observed properties of the present glasses in the background of the proposed model.

3.3. Molar Volumes. Compositions, densities, and molar volumes of the glasses are listed in Table 1. Molar volumes of the glasses were calculated from the experimental density. The variation of the V_{M} is plotted as a function of number of moles of oxygen in the molar formula in Figure 3. There is some scatter in the variation, particularly above 2.9 mol of oxygen. From the model, we expect the O^{2-} ion to be readily taken up by the P_2O_5 part of the network, and this results in the formation of metaphosphate units in the structure. If this has to happen locally by the modification of P−O−Ge bonds, it requires $[GeO_{4/2}]^0$ units to reorganize their connectivity in the structure, which we have discussed earlier. It results in the formation of Ge−O−Ge connections at the expense of P−O−Ge and ultimately, as Li_2O content is increased, the glass structure would gradually begin to appear as if it is mutually intergrown networks of GeO_2 and modified phosphate. This would naturally lead to more effective packing in space because the "openness" of the tetrahedral network of GeO_2 would be somewhat reduced by the interpenetration by metaphosphate chains. We have also calculated the molar volumes of the glasses using literature values of the molar volumes of $xLi_2O-zP_2O_5$ glasses,[28] subtracted these from the measured molar volumes, and obtained effective molar volumes of remaining GeO_2 glass. This is simply equal to $\Delta V = [V_{\mathrm{M}} - (x+z)\,V_{\mathrm{LP}}]$, where V_{LP} is the molar volume of the lithium−phosphate glass with a Li_2O/P_2O_5 ratio of x:z. $V_{\mathrm{eff(GeO2)}}$, which is $\Delta V/y$, thus calculated is indeed uniformly (significantly) lower (Table 2) than that of pure GeO_2 glass (28.40 cm^3), which supports the proposition that there is interpenetration of GeO_2 and phosphate networks.

Although the extent of modification is quite high in a number of glasses investigated here, we rule out random close packing (rcp) of O^{2-} ions as follows. Assume that all the oxygens in

TABLE 2: Effective Molar Volumes of GeO_2 in $Li_2O-GeO_2-P_2O_5$ Glasses

code	V_{LP}	$(x+z)\ V_{LP}$	V_M	ΔV	$V_{eff\ GeO2}\ (\Delta V/y)$
CPL1	53.05	26.53	34.16	7.63	15.26
CPL2	45.33	27.20	34.07	5.87	14.68
CPL3	40.29	28.20	32.48	4.28	14.27
CPL4	36.56	29.25	31.57	2.32	11.60
CPL5	33.75	30.38	31.61	1.23	12.30
CLG0	36.56	29.25	36.56		
CLG1	35.24	33.48	34.30	0.82	16.40
CLG2	33.75	30.38	31.61	1.23	12.30
CLG3	31.84	27.06	30.30	3.240	21.60
CLG4	30.27	24.22	28.73	4.51	22.55
CGP1	30.27	24.22	28.73	4.51	22.55
CGP2	36.56	29.25	31.57	2.32	11.60
CGP3	43.11	34.49	36.54	2.05	10.25

TABLE 3: Glass Transition Temperatures, Heat Capacities (at (T_g −20) K and Dulong-Petit), ΔC_P, ΔT_g, and $F_{1/2}$

sample	T_g (K)	C_p (at Tg−20K) ($JK^{-1}\ mol^{-1}$)	3nR ($JK^{-1}\ mol^{-1}$)	ΔC_p ($JK^{-1}\ mol^{-1}$)	ΔT_g (K)	$F_{1/2}$
CPL1	870					
CPL2	777					
CPL3	770					
CPL4	703	107.45	114.74		53	0.33
CPL5	655	112.09	114.74	61	50	0.33
CLG0	590	108.90	124.72	67	33	0.46
CLG1	626	109.59	119.73	49	39	0.42
CLG2	655	112.09	114.74	61	50	0.33
CLG3	681	107.99	109.75	67	49	0.35
CLG4	670	103.84	104.76	59	53	0.31
CGP1	670	103.84	104.76	59	53	0.31
CGP2	703	107.45	114.74	−	53	0.33
CGP3	710	115.78	124.72	61	66	0.24

the glass have an effective radius[29−31] of 1.36 Å, which is slightly larger than the bridging and nonbridging oxygen radii. The loose rcp volume is equal to $(4\pi r_0^3/3)\ (x + 2y + 5z)\ (6.023 \times 10^{23}*10^{-24}/0.6)$ cc. The P^{5+} and Ge^{4+} ions are assumed to pack into tetrahedral voids in the structure.[23] 3*N* tetrahedral voids are formed in rcp of *N* spheres. Since both Li^+ (0.67 Å) and Ge^{4+} (0.53 Å) are clearly larger than the radius of the tetrahedral void ($= 0.22r_0$) a volume corresponding to $(4\pi/3)\{2x((0.67)^3 - (0.22*1.36)^3) + y((0.53)^3 - (0.22*1.36)^3)\}\ (6.023 \times 10^{23}*10^{-24})$ cc has been added to the above rcp volume. We expect this corrected volume, V_{rcp}, to represent a higher estimate of the molar volumes. The variation of V_{rcp} is shown as a function of the number of oxygen atoms in the composition *N* $(= x + 2y + 5z)$ in Figure 3. The corresponding experimental molar volumes, V_M, are uniformly higher than even the V_{rcp}. This indicates that the glass structure, despite interpenetration of networks, is still sufficiently open, which is characteristic of covalently bonded network glasses. Presence of unmodified GeO_2 can provide such openness of structure. The structural model also anticipates that, except in the CPL1 composition, GeO_2, which remains as an unmodified component is integrated with the lithium phosphate glass, structurally at a molecular level. This integration is such as to prevent its phase separation. It is for this reason, that the molar volume calculated as the sum of $(V_{GeO2} + V'_{rcp})$ is closer to the experimentally observed V_M. The integration at a molecular level may involve the metaphosphate chain to integrate with the germania matrix and, therefore, may maximize the actual volume, which accounts for the experimentally observed molar volumes being closer to $V_{GeO2} + V'_{rcp}$.

3.4. Glass Transition. T_g values are listed in Table 3. The variation of T_g of all the glasses as a function of Li_2O concentration is shown in Figure 4a. Glass transition in this system is rather interesting for the following reasons. (1) Over the concentration regime investigated, there is a spread of 280 °K in T_g values. (2) Both binary lithium germanate and lithium

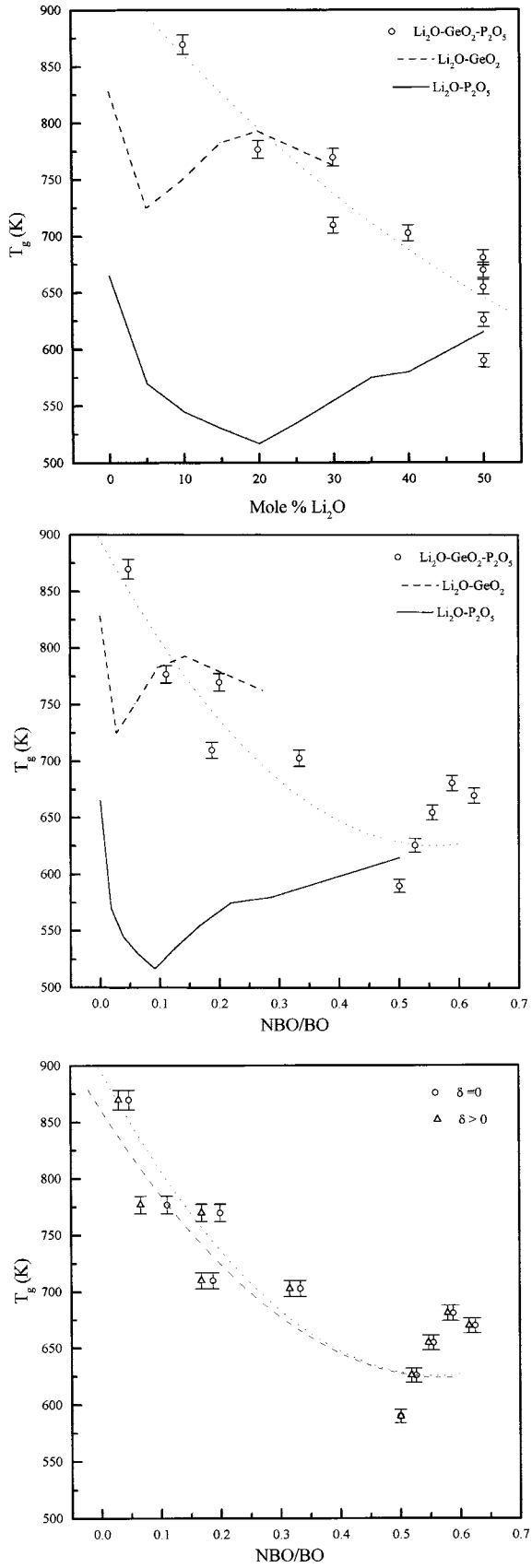

Figure 4. (a) Variation of T_g as a function of mole % Li_2O in the glass. (b) Variation of T_g as a function of NBO/BO ratio. (c) The effect of inclusion of δ on T_g vs NBO/BO plots.

phosphate glasses are known to exhibit atypical T_g variations as a function of Li_2O concentration. Li_2O-GeO_2 glasses exhibit a sharp minimum around 2 mol % Li_2O, above which T_g again rises sharply up to ~5 mol % Li_2O. Then it rises slowly to a maximum around 20 mol % Li_2O, above which it decreases only slightly up to 30 mol % Li_2O (limit of Li_2O concentration for easy glass formation).[32] $Li_2O-P_2O_5$ glasses, on the other hand exhibit a pronounced minimum of T_g around 20 mol % Li_2O, which rises toward 50 mol % Li_2O. T_g values exhibit a plateau above this concentration.[33] (3) The ternary $Li_2O-GeO_2-P_2O_5$ glasses exhibit T_g significantly higher than either $Li_2O-P_2O_5$ or Li_2O-GeO_2 glasses, particularly when less than 20 mol % Li_2O is present. Above this concentration, T_g are almost as high as those of the binary germanate glasses, which are much higher than those of binary phosphate glasses. In Figure 4a, the T_g behavior of binary $Li_2O-P_2O_5$ and Li_2O-GeO_2 glasses taken from the literature[32,33] are shown for comparison. Ternary glasses exhibit a generally decreasing trend in T_g as a function of Li_2O. The presence of even small proportions of GeO_2 appears to increase the glass transition temperature as is evident in CLG series.

On the basis of the structural model, the T_g behavior as a function of Li_2O in binary Li_2O-GeO_2 glass can be understood as a result of three distinct stages of structural changes.[32] Up to 5 mol % of Li_2O, there is the formation of both NBO and six-coordinated germanium ($[GeO_{6/2}]^{2-}$). The initial drop in T_g appears to be due to formation of NBOs, which quickly rises again above 2 mol % due to the formation of $[GeO_{6/2}]^{2-}$. Between 5 and 20 mol % Li_2O, the dominant effect seems to be due to strengthening of the structure by six-coordinated germanium as more bridging oxygens (BOs) are formed. Decrease of T_g above approximately 20 mol % Li_2O concentration appears to be due to preferential formation of NBOs. In Rb_2O-GeO_2 binary glasses, the formation of both NBO and $[GeO_{6/2}]^{2-}$ has been established quantitatively using a combination of XPS and EXAFS studies.[9] It is fair to assume from this study that $[GeO_{6/2}]^{2-}$ and NBOs are formed in the region up to 20 mol % of alkali, whereas the concentration of $[GeO_{6/2}]^{2-}$ rapidly declines above 20 mol % alkali. In binary alkali phosphate glasses, however, adding Li_2O quite simply results in the formation of NBOs and progressive degradation of ultraphosphate ($[POO_{3/2}]^0$) to meta- ($[POO_{2/2}O]^{-1}$), pyro- ($[POO_{1/2}O_2]^{-2}$), and ortho- ($[POO_3]^{-3}$) phosphates, in that order. The gradual increase in T_g (beyond ~20 mol % alkali), despite network degradation in $Li_2O-P_2O_5$ glasses, is considered to be a consequence of the strong coordination of Li^+ ions to oxygens of the phosphate species,[33] which results in cross linking and increased structural strength of the glass. We may recall that lithium ions have a large charge-to-radius ratio, which results in a relatively strong polarization and bonding with NBOs. The variation of T_g in both of the binaries is thus atypical in the sense that T_g does not decrease monotonically as a function of Li_2O concentration.

There are also significant differences in the Li_2O concentration ranges of the two binaries in the present glass system. It would, therefore, be beneficial to discuss variation of T_g as a function of NBO/BO ratios rather than of Li_2O concentrations. The evaluation of the NBO/BO ratio is complicated because of the tendency of GeO_2 glasses to form $[GeO_{6/2}]^{2-}$ units. In the absence of this tendency it is easy to see that, in an $xLi_2O + (1 - x)$ GeO_2 glass, the NBO/BO ratio, R_{Ge}, is simply $2x/(4 - 6x) = x/(2 - 3x)$. If δ O^{2-} (δ is also in mole fraction units such as x) is expended in forming $[GeO_{6/2}]^{2-}$, which increases the BOs by 2δ and decreases NBOs by 2δ, this ratio becomes $[(x - \delta)/(2 - 3x + \delta)] = R'_{Ge}$. We note that $R'_{Ge} < R_{Ge}$ for $\delta > 0$. For the case of binary $xLi_2O + (1 - x)P_2O_5$ glasses, the ratio is simply $R_P = [x/(3 - 4x)]$. In the ternary germanophosphate glasses, it is difficult to estimate the NBO/BO ratio because of the uncertainty in the tendency of $[GeO_{4/2}]^0$ to acquire O^{2-} and form $[GeO_{6/2}]^{2-}$. We assume that δ GeO_2 values of Jain et al.[9] can be used as an approximation. Addition of xLi_2O generates $2x$ or $(2x - 2\delta)$ NBOs in the structure. The net BOs will be $(4y + 6z - 2x)$ or $(4y + 6z - 2x + 2\delta)$, and the ratio of NBO/BO will be $[x/(2y + 3z - x)]$ or $[(x - \delta)/(2y + 3z - x + \delta)]$. The variation of T_g as a function of NBO/BO ratio is shown in Figure 4b for both binaries and the present ternary glasses without the use of δ. When determining the values of δ in ternary glasses it is tentatively assumed that the relevant modifier concentration is $(xy/(x + y))$, and not just x. When T_g are plotted as a function of NBO/BO, calculated in this manner, there appears to be monotonic decrease of T_g in the ternary $Li_2O-GeO_2-P_2O_5$ glasses. The atypical T_g behavior observed in both lithium-germanate and lithium-phosphate glasses is absent in lithium-germanophosphate glasses. When use was made of the NBO/BO ratio calculated using δ from the literature,[9] the nature of T_g variation is found to be not much affected as shown in Figure 4c. Thus, T_g behavior as a function of NBO/BO does not seem to be very sensitive to the presence of $[GeO_{6/2}]^{2-}$ units in the ternary glass structure. However, the glass transition temperatures of the germanophosphate glasses are greater than the T_g of the component binary glasses in most of the compositions. This has importance in technological applications of germanophosphate glasses. The glass transition temperatures are closer to, and in some cases are even higher than, those of GeO_2 glass itself because the rigidity of the matrix is indeed expected to be even higher than in GeO_2 itself. This is because the voids of the open structure of GeO_2 glass are somewhat stuffed by the interpenetrating metaphosphate chains. The increased stiffness has the effect of elevating the glass transition temperature.

3.5. Heat Capacities. The heat capacities generally exhibit step-like change at T_g. In Table 3, molar heat capacities measured at $(T_g - 20)$ K are listed along with the ΔC_p values. The uncertainty in ΔC_p values is somewhat large (~10−20%). The Dulong−Petit (3nR) heat capacities, calculated on the assumption that all the vibrational modes are excited below T_g, are also listed in Table 3. It may be noted that in glasses with high GeO_2 and low Li_2O (see CPL series) it was not possible to do measurements on DSC, and hence ΔC_p have not been determined. T_g values were, however, determined using DTA measurements and are listed in Table 3. In general C_p values at $(T_g - 20)$ K are uniformly lower than the Dulong-Petit heat capacities. This is because the vibrational modes are not fully excited in the network. In the present glass structure, the presence of several entities such as metaphosphate and pyrophosphate units, appears to lead to a large density of configurational states in the liquid just above T_g. The sudden accessibility of a large density of glassy minima, in the supercooled regime gives rise to large configurational entropy, and hence the large ΔC_p values compared to other phosphate glasses.[25,34,35] It also reveals that these glasses are quite fragile since ΔC_p correlates directly to fragility.[36] There is as yet no prescription in the literature to correlate the kinetic fragilities of multicomponent glasses, such as germanophosphates, to any of the molecular properties of component binaries. Kinetic fragilities ($F_{1/2}$) can, however, be evaluated following the recently proposed definition by Ito et al.[19]

$$F_{1/2} = (0.151T_g - \Delta T_g)/(0.151T_g + \Delta T_g)$$

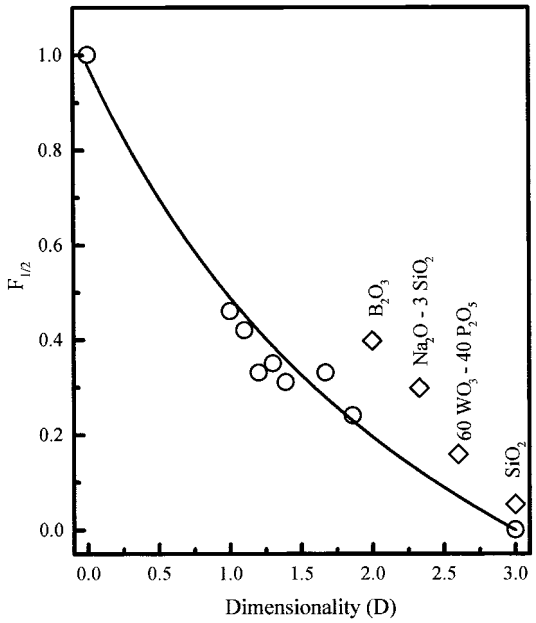

Figure 5. Variation of kinetic fragility ($F_{1/2}$) as a function of dimensionality (D).

because T_g and ΔT_g values are experimentally measured. These values of $F_{1/2}$ are given in Table 3 for all of the glasses. The structural model of the glasses can be used effectively to understand the fragility behavior. The model suggests that the strong component GeO_2 remains unaffected, while the (relatively fragile) P_2O_5 gets modified and becomes more fragile due to network degradation. There is, at present, no prescription for $F_{1/2}$ fragilities of complex systems containing two network formers to any other macroscopic or molecular properties of the glass. In general, we note that the physical (network) dimensionalities of the glass formers and their fragilities are covariant. Thus, the three-dimensionally connected network glass formers, such as SiO_2 and GeO_2, are stronger than two-dimensionally connected glass formers, such as P_2O_5 and B_2O_3. The fragilities may then be examined in the light of the spatial dimensionalities, D, of the glasses. We find an approximate relation, between $F_{1/2}$ and D as

$$F_{1/2} = 0.98(3 - D)/(3 + D)$$

D in this expression is the mole fraction weighted dimensionality of the glass composition. In the present case, for example, P_2O_5 (unmodified) has a dimensionality 2, metaphosphate ($\equiv [PO_{3/2}O]^{1-}$) has a dimensionality 1, pyrophosphate ($\equiv [PO_{2/2}O_2]^{2-}$) has zero, and $[GeO_{4/2}]^0$ has a dimensionality 3, which is same as of $[GeO_{6/2}]^{2-}$. The behavior of $F_{1/2}$ as a function of D is shown in Figure 5, where the solid line represents the function $0.98(3 - D)/(3 + D)$. We have found that the fragilities of several other glasses reported in the literature are consistent with the above function. For example, the points marked by □ are the fragilities taken from references[19,34] and plotted against similarly calculated dimensionalities.

Because in the present system of glasses GeO_2 is expected to remain unaffected according to the suggested model and, therefore, has a dimensionality equal to 3, and these values lie on fragility function, it is an indirect evidence for the validity of the structural model. We may also add that whenever there is a glass formed with strong and fragile glass formers, modification is more likely to occur on the more fragile part. Also in such strong-fragile mixed former systems, the glass transition is determined by the strong former.

3.6. IR Spectra. IR spectra of all the glasses investigated in this work are presented in Figure 6a−c. The spectra are generally dominated by features attributable to the phosphate units. The spectra of the CGP series of glasses reveal some characteristic features. In two glasses, where the Li_2O/P_2O_5 ratio is less than or equal to 1 and P_2O_5 content itself is ≥ 40 mol %, the IR peak in the 1200−1260 cm^{-1} region, which is attributable to P = O appears well delineated and dominant. This is followed by symmetric and asymmetric modes of PO_4 tetrahedra in the 1100 cm^{-1} region.[37−39] In CGP1, where Li_2O is 50 mol % and the concentration of P_2O_5 is only 30 mol %, the P═O peak merges into the shoulder [PO_4] group frequencies and is not clearly identifiable.[40] The features above 1000 cm^{-1} can be attributed to the symmetric and asymmetric stretching of the PO_4 groups in these glasses.[37−39] The peak around 920 cm^{-1} does not change much with composition and is likely to arise from GeO_4 tetrahedra,[13,41] as these are for constant GeO_2 glasses. The 750 cm^{-1} feature intensifies with increasing percentage of P_2O_5 and therefore is attributable to P−O−P stretching mode.[37−39] The sharp feature at 668 cm^{-1} and a similar feature at 2347 cm^{-1} (not shown in the figure) are present in all of the glasses and are attributed to CO_2 modes,[42] which occur due to the instrumental limitations. There is a fairly strong absorption band that broadens and red shifts significantly from 570 cm^{-1} to 500 cm^{-1} with increasing proportion of P_2O_5 content. This arises from a combination of P−O−Ge and P−O−P bending modes in these glasses with constant GeO_2 content. Dominance of P−O−Ge bending may account for the apparent red shift. The 450 cm^{-1} feature, which disappears in CGP3 containing low Li_2O content, is likely to be due to P−O−Ge bending, which may be present only in high Li_2O glasses.

The spectra of CPL series of glasses reveal profound structural changes with composition. The CPL1 spectra consist of the P═O stretching peak above 1200 cm^{-1}, but only as a broad shoulder peaking at 1260 cm^{-1}. In other compositions, it occurs between 1216 and 1228 cm^{-1}. The two peaks at 1092 and 1028 cm^{-1} are attributable to symmetric and asymmetric stretching in PO_4 tetrahedra.[37−39] The 936 cm^{-1} peak is likely to arise from the overlap of vibrational modes of GeO_4 tetrahedra and asymmetric P−O−P stretching modes. The symmetric P−O−P stretching modes appear as a shoulder around 770 cm^{-1}. The bending modes of P−O−P and P−O−Ge again appear in the region of around 525 and 470 cm^{-1}, although they are not as well defined. There is one unique absorption feature in the spectra of CPL1 glass, which is absent in the spectra of all other glasses. There is a well-defined shoulder around 802 cm^{-1}. We tentatively attribute it to the asymmetric stretching of GeO_6 octahedra.[13,41] In the other glasses of this series, features corresponding to P═O and the P−O−P stretching appear as well-defined peaks.

In the CLG series, variations of the phosphate-related vibrations are somewhat similar to those of CPL series because Li_2O/P_2O_5 ratio increases in both cases down the series (see Table 1). P═O vibrations are not clearly delineated in CLG0, and it may be due to an already high level of modification.[40] Since there is no other vibrational band with similar energy, the P−O−P bending mode at 480 cm^{-1} appears well defined and is intense. The P−O−P stretching modes are split when GeO_2 concentration is very low, which may be due to differences arising from the incorporation of $[GeO_{4/2}]^0$ into the network, which introduces new P−O−Ge modes. However, as the GeO_2 concentration increases, most of the peaks become sharp and well defined, and the P−O−P stretching, in particular, becomes

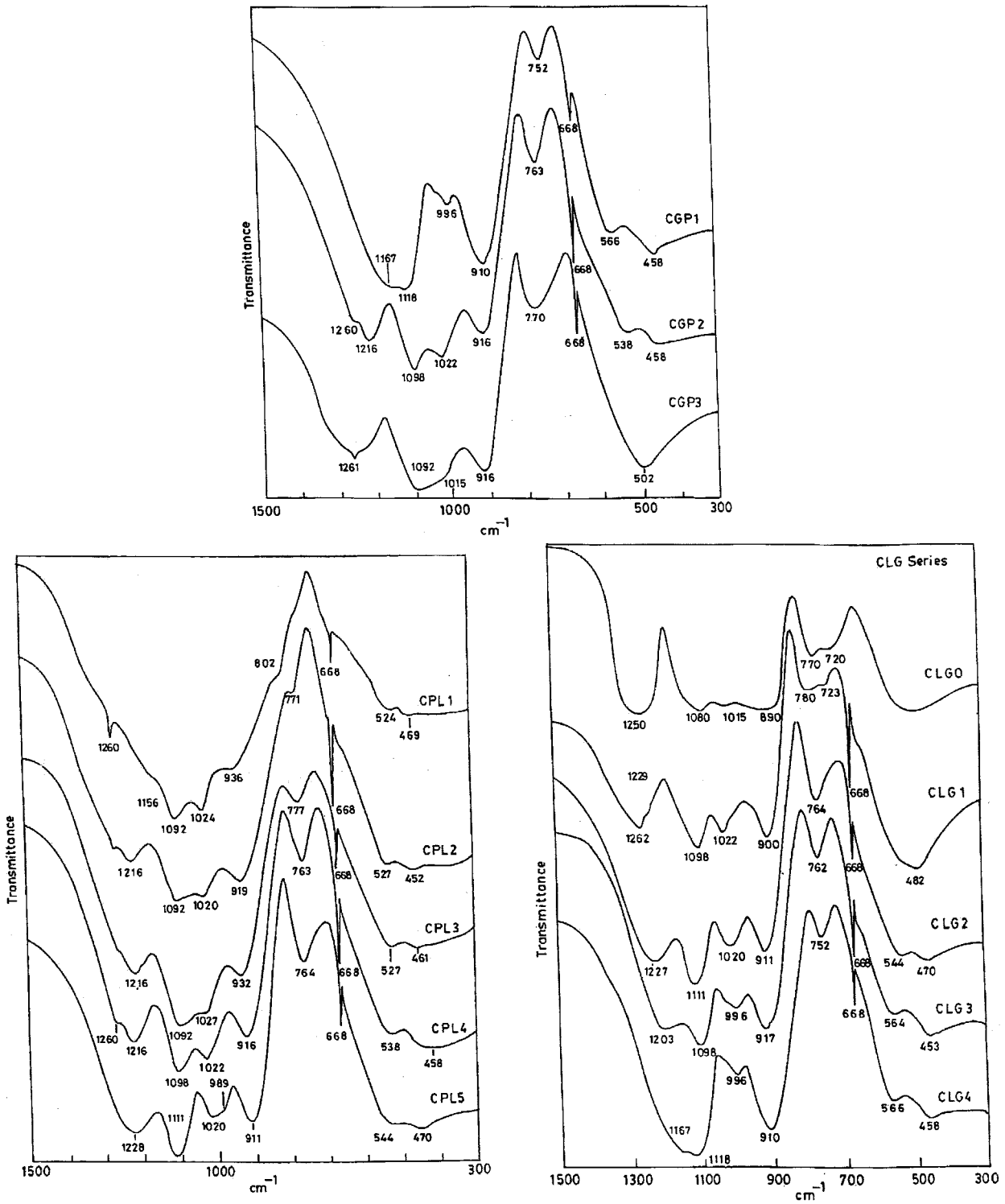

Figure 6. Infrared spectra of (a) CGP, (b) CPL, and (c) CLG series of glasses.

notably sharp. The absorption features, which occur in the region of 450−570 cm^{-1}, arise from both P−O−P and P−O−Ge bending modes.[13,41] Thus, except in CPL1, there is no feature attributable to changes in vibrational modes (∼920 cm^{-1}) of $[GeO_{4/2}]^0$groups, which is consistent with the structural model.

3.7. Raman Spectra. Raman spectra of all the glasses are shown together in Figure 7a−c. In the CGP series, features due to phosphate undergo drastic changes. The peak around 1000 cm^{-1}, attributable to pyrophosphate groups in CGP1, disappears in CGP2 and CGP3. In CGP3, the relatively intense 1300 cm^{-1} peak could be due to P═O as it is an ultraphosphate composition. Ge−O−P stretching frequencies are observed around 750 cm^{-1} and Ge−O−P bending vibrations around 580 cm^{-1}.[13,43−45]

In the CPL series, phosphate-related vibrations are seen around 1260 cm^{-1} (P═O), and symmetric stretching of PO_4 tetrahedra at 1118−1153 cm^{-1}.[43−45] The 960 cm^{-1} peak is associated with symmetric stretching in $[GeO_{4/2}]^0$ units,[13] whereas the 777 cm^{-1} peak is due to the stretching of Ge−O−P bridges.[13] There is a 643 cm^{-1} feature in the spectra of only CPL1. We attribute this unique feature to Ge_6−O−P bending modes,[13] which is higher than the frequencies corresponding to Ge_4−O−P bending modes at 575 cm^{-1}; the latter

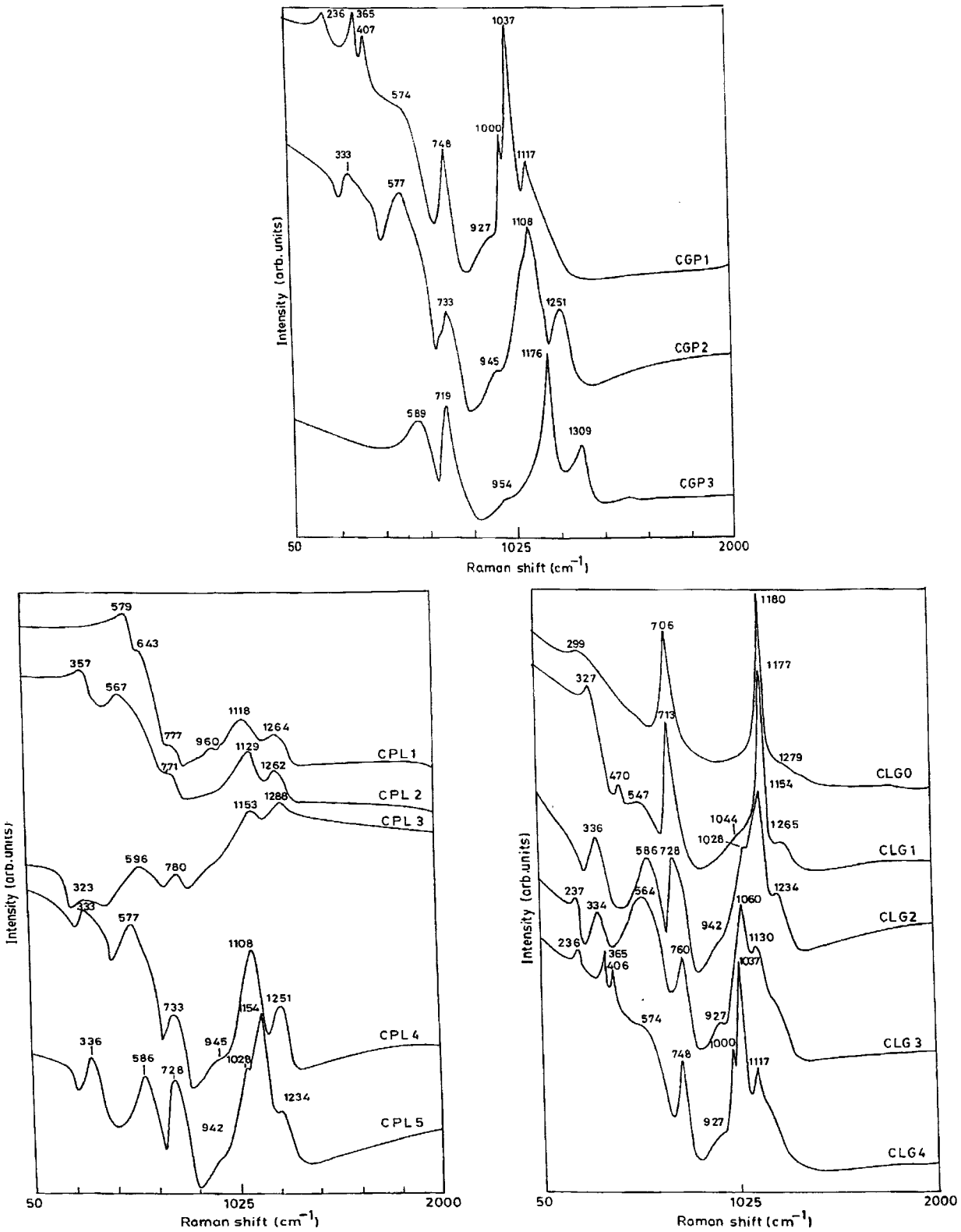

Figure 7. Raman spectra of (a) CGP, (b) CPL, and (c) CLG series of glasses.

is present in all glasses (Ge_6 represents Ge in six coordinated $[GeO_{6/2}]^{2-}$ units in the structure). The high value of the bending frequencies is understandable because in Ge_6-O-P there is a greater crowding of O due to GeO_6 groups, which makes Ge−O−P bending more difficult. These frequencies vary in the expected manner when the modification (Li_2O) increases and GeO_2 concentration decreases because the relative intensities of the 570 cm^{-1} peak decrease rapidly and the P═O feature also gets reduced in clarity and intensity.

The spectra of CLG0 is the simplest and is due to lithium metaphosphate consisting of symmetrical stretching features of PO_4 tetrahedra at 1180 cm^{-1} and P−O−P stretching at 706 cm^{-1}. There is a weak feature at 1279 cm^{-1} due to P═O. The feature around 570−580 cm^{-1}, due to Ge−O−P bending, emerges as a strong feature when the GeO_2 concentration increases and there is no indication of the presence of GeO_6. The vibrational features of the phosphate group in the region between 1000 and 1200 cm^{-1} remain intense, and the subpeaks

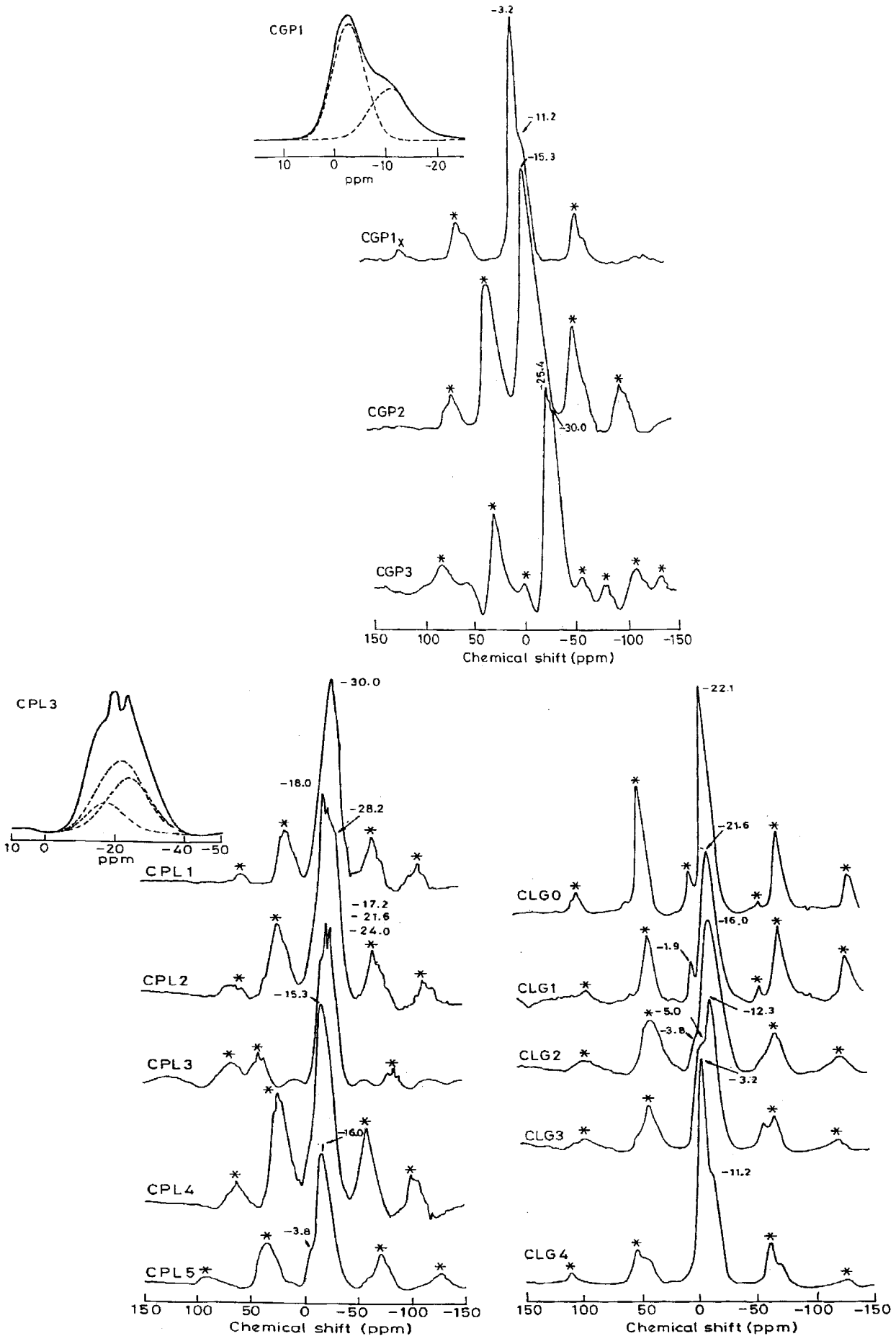

Figure 8. ^{31}P MAS NMR of (a) CGP, (b) CPL, and (c) CLG series of glasses.

TABLE 4: ^{31}P Chemical Shift Values of $Li_2O-GeO_2-P_2O_5$ Glasses

	chemical shifts (ppm)		
sample	ultra	meta	pyro
CPL1	−30.0		
CPL2	−28.2	−18.0	
CPL3		−17.2	
		−21.6	
		−24.0	
CPL4		−15.3	
CPL5		−16.0	−3.8
CLG0		−22.1	
CLG1		−21.6	−1.9
CLG2		−16.0	−3.8
CLG3		−12.3	−5.0
CLG4		−11.2	−3.2
CGP1		−11.2	−3.2
CGP2		−15.3	
CGP3	−30.0	−25.4	

in this region reflect an increase in the degree of modification. Formation of pyrophosphate is indicated, particularly in CLG4 by the absorption at 1000 cm^{-1}. The features in the region of 920−950 cm^{-1} are attributable to P−O−Ge stretching and also to modes in $[GeO_{4/2}]^0$ units.[13]

In all of the glasses, a relatively broad peak is seen around 350 cm^{-1}, which is attributable to cage vibrational frequencies of Li^+ ions, as noted in earlier studies of lithium ion containing glasses.[46]

The IR and Raman spectroscopic features are all consistent with the structural model. This includes the unique feature in the CPL1 spectra, which is attributable to the presence of $[GeO_{6/2}]^{2-}$ units, envisaged by the model. Because it is also known that in binary Li_2O-GeO_2 glasses $[GeO_{6/2}]^{2-}$ is present up to 20 mol % Li_2O, we have drawn line in Figure 1 that connects 10% Li_2O to 20% Li_2O on the Li_2O-GeO_2 line. The line is open on the higher P_2O_5 side as $[GeO_{6/2}]^{2-}$ has not been observed in these compositions. This tentatively represents the upper composition bound to the formation of $[GeO_{6/2}]^{2-}$ in the present ternary system. Although the model accounts for all of the observed phosphatic species from the MAS NMR studies, there are four compositions (CLG1, CLG2, CLG3, and CLG4) in which $[GeO_{3/2}O]^{1-}$ units are expected to form *only if eq 3 or eq 5 were to operate*. Because they are not observed experimentally, we have suggested that Li_2O finds itself preferentially solubilized into metaphosphate regions and continues to modify only the phosphate by reaction 4.

3.8. ^{31}P-MAS NMR Studies. ^{31}P spectra of all the glasses investigated in this work are shown in Figure 8a−c. The chemical species identified on the basis of ^{31}P resonance peaks (as due to ultra-, meta-, and pyrophosphate groups) are listed in Table 4 against the glass composition.[47−49] The ultra-, meta-, and pyrophosphate units are designated in the present NMR studies as P_3, P_2, and P_1 respectively, where the subscript indicates the number of BOs connected to phosphorus atom. Because in most compositions we expect more than one phosphate species to be present and also because the signals from various species overlap significantly, the full widths at half-maximum (fwhm) of these peaks have not been listed nor have they been analyzed any further. However, in all cases, the MAS NMR peaks have been deconvoluted using a "peakfit: program in order to identify the species and their chemical shift values. In the case of pure metaphosphate glass, CLG0, the resonance is very sharp and occurs at −22.1 ppm. With the addition of GeO_2, the fwhm of the peaks are affected significantly, for example, in CPL4, which may be regarded as a lithium metaphosphate glass with 20 mol % GeO_2, the fwhm of the metaphosphate resonance is considerably broader and is also highly deshielded (chemical shift −15.3 ppm) compared to the same in CLG0 metaphosphate glass at −22.1 ppm.

In the CPL series, the MAS NMR of ^{31}P in CPL1 is unique. Only a single broad resonance is observed at a chemical shift of −30 ppm. Despite the presence of 10 mol % Li_2O, the presence of a single ^{31}P resonance, can be attributed to the phosphorus atom in ultraphosphate species P_3. Such a possibility is in consonance with the IR and Raman studies also indicated the presence of $[GeO_{6/2}]^{2-}$ units in the structure of CPL1 (and only CPL1). In CPL2, we observed a combination of P_3 and P_2 centered around −28.2 and −18.0 ppm. The P_2 signal appears split because phosphorus is present with two types of second neighbor connectivities in P−O−Ge as well as P−O−P. The oxygen in $[GeO_{4/2}]^0$ carries more negative charge than the oxygen in $[POO_{3/2}]^0$ and therefore they bring about different degrees of shielding of ^{31}P. It may be noted that P_3 appears only as a shoulder. In CPL3, P_3 does not seem to be present but only P_2 is seen, which is triply split. We attribute this to the influence of second neighbors of the phosphorus atom in P_2, which could be two phosphorus atoms, one phosphorus and one germanium, or both germanium atoms, which result in slightly different values of chemical shift. CPL4, as pointed out earlier, gives rise to a single ^{31}P signal due to metaphosphate units. This is evidently more shielded and the resonance peak is also broader. There is much intensity in the sidebands, suggesting large asymmetry of the sites in most of the cases. CPL5 also exhibits two signals, one of which is of lower intensity and occurs with a chemical shift of −3.8 ppm. It is most likely due to the ^{31}P in pyrophosphate units.

Glasses of the CLG series all exhibit twin signals corresponding to meta- and pyrophosphate, and the intensity of pyrophosphate increases as the extent of modification increases. CGP series, in which GeO_2 content is held constant, gives rise to resonance of pyro and metaphosphate in CGP1 and meta and ultraphosphate in CGP3. However, CGP2 (same as CPL4) exhibits only metaphosphate signals.

Thus, the MAS NMR of germanophosphate glasses is consistent with the hypothesis that Li_2O modifies preferentially only the P_2O_5 part of the glass; otherwise, Li_2O would be insufficient to lead to the formation of P_2 and P_1 species found in several glasses. Together with the IR and Raman spectroscopic observations, we infer that the GeO_2 part of the glass remains unaffected in all of the compositions. Germanophosphate glass behaves as if it is a glass formed from a solution of GeO_2 and lithium−phosphate glass with $[GeO_{4/2}]^0$ units or $[GeO_{4/2}]^0_n$ network fragments, and P_3, P_2, and P_1 units are randomly integrated (interwoven) in the structure.

4. Conclusions

Lithium germanophosphate glasses ($xLi_2O-yGeO_2-zP_2O_5$) have been synthesized over a wide range of compositions and their thermal and spectroscopic behavior have been investigated. IR and Raman spectroscopies indicate that, except in $10Li_2O-50GeO_2-40P_2O_5$ glass, there is no evidence of the formation of $[GeO_{6/2}]^{2-}$ in any of the glasses, and hence no evidence of germanate anomaly, where P_2O_5 is present in the glass system. In CPL1, however, there is a plausible thermodynamic justification for the formation of $[GeO_{6/2}]^{2-}$ units. In IR spectra of CPL1, a feature at 802 cm^{-1}, is attributed to the stretching mode of $[GeO_{6/2}]^{2-}$ units. Similarly, in the Raman spectra of CPL1 also, a unique feature, around 643 cm^{-1}, is attributed to the bending modes of Ge$_6$−O−P. ^{31}P MAS NMR studies suggest that the

formation of ultra-, meta-, and pyrophosphate species is consistent with modification of only the P_2O_5 part of the glass. Therefore, in a glass containing a strong (GeO_2) and fragile (P_2O_5) formers, the modification seems to take place predominantly only on the fragile component. A structural model has been developed, which is consistent with the observed properties. The presence of $[GeO_{6/2}]^{2-}$ units in CPL1 is shown to be a consequence of relative thermodynamic stability. The properties have been analyzed keeping in view that the glasses may be considered as pseudo binaries of $y GeO_2$ and $xLi_2O-zP_2O_5$ glasses. The molar volumes of the glasses are found to be higher than the corresponding rcp volumes, but lower than the simple sum of the molar volumes of component GeO_2 and $Li_2O-P_2O_5$ glasses. Some interpenetration of the GeO_2 and phosphate networks appears evident. The glass transition temperatures of these ternary glasses show a trend, which is different from the trend of component binaries, and exhibit a decreasing trend with increasing NBO/BO ratio. The T_g values are also higher than either of the component binaries up to ~20 mol % GeO_2. This aspect may be technologically very important. In strong−fragile mixed glass former system, T_g are determined by the "strong" component.

$F_{1/2}$ (kinetic) fragilities of these glasses have been calculated, and it is shown that $F_{1/2}$ has a functional dependence on the physical dimensionality (D), i.e., $F_{1/2} = 0.98\,(3 - D)/(3 + D)$, where D is the mole fraction weighted dimensionality.

Acknowledgment. One of us (S.K.) is grateful to the Council for Scientific and Industrial Research (CSIR), India, for the research fellowship. S.M. is thankful to the Commission of the European Communities for financial support. We acknowledge the useful discussions with Mr. Harish Bhat.

References and Notes

(1) Murthy, M. K.; Kirby, E. M. *Phys. Chem. Glasses* **1964**, *5*(5), 144−146.
(2) Sakka, S.; Kamiya, K. *J. Noncryst. Solids*. **1982**, *49*, 103−116.
(3) Mundy, J. N.; Jin, G. L. *Solid State Ionics*. **1986,** *21*, 305−325.
(4) Murthy, M. K.; Ip, *J. Am. Ceram. Soc*. **1964**, *47*, 328.
(5) Murthy, M. K.; Aguayo, *J. Am. Ceram. Soc*. **1964**, *47*, 444.
(6) Murthy, M. K.; Long, L.; Ip, *J. Am. Ceram. Soc*. **1968**, *51*, 661.
(7) Evstropev, K. K.; Pavlovskii, V. K. *Inorg. Mater*. **1967**, *3*, 592.
(8) Henderson, M. K.; Fleet, M. E. *J. Non-Cryst. Solids* **1991**, *134*, 259−269.
(9) Huang, W. C.; Jain, H.; Marcus, M. A. *J. Non-Cryst. Solids* **1994**, *180*, 40−50.
(10) Huang, W. C.; Jain, H.; Meitzner, G. *J. Non-Cryst. Solids* **1996**, *196*, 155−161.
(11) Lu, X.; Jain, H.; Huang, W. C. *Phys. Chem. Glasses* **1996**, *37*(5), 201−205.
(12) Osaka, A.; Jianrong, Q.; Miura, Y.; Yao, T. *J. Non-Cryst. Solids* **1995**, *191*, 339−345.
(13) Kamitsos, E. I.; Yiannopoulos, Y. D.; Karakassides, M. A.; Chryssikos, G. D.; Jain, H. *J. Phys. Chem*. **1996**, *100*, 11755−11765.
(14) Kamitsos, E. I.; Yiannopoulos, Y. D.; Varsamis, C. P.; Jain, H. *J. Non-Cryst. Solids* **1997**, *222*, 59−68.
(15) Durban, D. J.; Wolf, G. H. *Phys. Rev. B* **1991**, *43*, 2355.
(16) Price, D. L.; Ellison, A. J. G.; Saboungi, M. L.; Hu, R. Z.; Egami, T.; Howells, W. S. *Phys. Rev. B* **1997**, *55*(17), 11249.
(17) Hussin, R.; Holland, D.; Dupree, R. *J. Non-Cryst. Solids* **1998**, *232−234*, 440−445.
(18) Rao, K. J.; Baskaran, N.; Ramakrishnan, P. A.; Ravi, B. G.; Karthikeyan, A. *Chem. Mater*. **1999**, *10*, 3109−3123.
(19) Ito, K.; Moynihan, C. T.; Angell, C. A. *Nature* **1999**, *398*, 492−495.
(20) Sathyanarayana, D. N. *Vibrational Spectroscopy − Theory and Applications*; New Age International Publishers: New Delhi, 1996; pp 62−63.
(21) Muthupari, S.; Rao, K. J. *J. Phys. Chem*. **1994**, *98*, 2646.
(22) Sanderson, R. T. *Polar Covalence*; Academic Press: New York, 1983.
(23) Ganguli, M.; Rao, K. J. *J. Non-Cryst. Solids* **1999**, *243*, 251−267.
(24) Ganguli, M.; Rao, K. J. *J. Phys. Chem. B* **1999**, *103*, 920−930.
(25) Selvaraj, U.; Rao, K. J. *J. Non-Cryst. Solids* **1988**, *300*, 104.
(26) Johari, G. P. *J. Chem. Phys.* **2000**, *112*, 8958.
(27) Pauling, L. *Nature of the Chemical Bond*; **1960**, Cornell University Press: New York.
(28) Mazurin, O. V.; Streltsina, M. V.; Shvaiko-Shvaikovskaya, T. P. *Handbook of Glass Data*; Elsevier: Amsterdam, 1985.
(29) Cargill, G. S. *J. Appl. Phys.* **1970**, *41*, 2248.
(30) Finney, J. L. *Nature* **1977**, *266*, 309.
(31) Cohen, M. H.; Turnbull, D. *Nature* **1964**, *203*, 964.
(32) Shelby, J. E.; Ruller, J. *Phys. Chem. Glasses* **1987**, *28*(6), 262−268.
(33) Hudgens, J. J.; Brow, R. K.; Tallant, D. R.; Martin, S. W. *J. Non-Cryst. Solids* **1998**, *223*, 21−31.
(34) Selvaraj, U.; Sundar, H. G. K.; Rao, K. J. *J. Chem. Soc., Faraday Trans I*. **1989**, *85*, 251−267.
(35) Sobha, K. C.; Rao, K. J. *J. Non-Cryst. Solids* **1996**, *201*, 52−65.
(36) Xia, X.; Wolynes, P. G. *Cond-mat.* /9912442.
(37) Corbridge, D. E. C.; Lowe, E. J. J. *J. Chem. Soc*. **1954**, 493.
(38) Almeida, R. M.; Mackenzie, J. D. *J. Non-Cryst. Solids* **1980**, *40*, 535.
(39) Hudgens, J. J.; Martin, S. W. *J. Am. Ceram. Soc*. **1993**, *76*, 1691.
(40) Brow, R. K.; Tallant, D. R.; Hudgens, J. J.; Martin, S. W.; Irwin, A. D. *J. Non-Cryst. Solids* **1994**, *177*, 221.
(41) Margaryan, A.; Piliavin, M. A. *Germanate Glasses: Structure, Spectroscopy and Properties*; Artech House: Boston, 1993.
(42) Rao, C. N. R. *Chemical Applications of Infrared Spectroscopy*; Academic Press: New York, 1963; p 621.
(43) Krimi, S.; Jazouli, El.; Rabardel, L.; Couzi, M., Mansouri, I.; Flem, G. El. *J. Solid State Chem*. **1993**, *102*, 400.
(44) Nelson, C.; Tallant, D. R. *Phys. Chem. Glasses* **1984**, *25*, 31.
(45) Tatsumisago, M.; Kowada, Y.; Minami, T. *Phys. Chem. Glasses* **1988**, *29*, 63.
(46) Tarte, P. *Spectrochim. Acta* **1964**, *20*, 238.
(47) Brow, R. K.; Kilpatrick, R. J.; Turner, G. L. *J. Non-Cryst. Solids* **1990**, *116*, 39.
(48) Villa, M.; Carduner, K. R.; Chiodelli, G. *J. Solid State Chem*. **1987**, *69*, 19.
(49) Prabakar, S.; Rao, K. J.; Rao, C. N. R. *Chem. Phys. Lett*. **1987**, *139*, 96.